Bridging the Gap Between Graetz's and Lévêque's Analyses for Mass/Heat Transfer in a Channel with Uniform Concentration or Flux at the Wall

João P. Lopes
Dept. of Chemical Engineering, Laboratory of Separation and Reaction Engineering, Associate Laboratory LSRE/LCM, Faculty of Engineering, University of Porto, Portugal

Silvana S.S. Cardoso
Dept. of Chemical Engineering and Biotechnology, University of Cambridge, U.K

Alírio E. Rodrigues
Dept. of Chemical Engineering, Laboratory of Separation and Reaction Engineering, Associate Laboratory LSRE/LCM, Faculty of Engineering, University of Porto, Portugal

DOI 10.1002/aic.12719
Published online July 22, 2011 in Wiley Online Library (wileyonlinelibrary.com).

A new approximate solution which bridges the gap between the classical theories of Graetz and Lévêque for heat/mass transfer in channel flow is presented. The results include expressions, uniformly valid in the axial direction, for the mixing-cup concentration (or temperature) profile $\langle c \rangle$ when transport towards the wall is slow (Dirichlet limit), and for the Sherwood number Sh when the wall flux can be considered uniform (Neumann limit). The technique employed provides insight into the mathematical structure of both quantities $\langle c \rangle$ (or conversion X_R) and Sh identifying explicitly the contributions from fully developed and developing behaviors, while maintaining accuracy in the transition region. Criteria to bound the different convection-diffusion regimes are suggested, which critically systematize previous results. These results are important for model selection in the design and simulation, among others, of heat exchangers and wall-coated microreactors where fast heterogeneous reactions occur. © 2011 American Institute of Chemical Engineers *AIChE J,* 58: 1880–1892, 2012

Keywords: mathematical modeling, heat transfer, mass transfer, Graetz problem, Lévêque's solution

Introduction

Modeling heat or mass transfer in internal channel flow has been the basis for analyzing heat exchangers and tubular chemical reactors, being therefore of utmost importance for the understanding of a large number of chemical engineering processes. For a channel with high length-to-diameter ratio, in the absence of bulk source terms, the conservation equation translates the balance between convective transport and transfer to or from the wall. This can be formulated as the classical Graetz-Nusselt problem,[1,2] which has been extensively dealt in the literature for several boundary conditions at the channel's surface (suitable reviews are available in the literature[3–6]). The simplest cases include the situations of uniform temperature (concentration) or uniform heat (mass) flux evaluated at the wall, Dirichlet and Neumann boundary conditions respectively. In heat exchangers, these boundary conditions can be found when the fluid conductivity is much smaller or larger than the wall conductance. In chemical reactors, a fast heterogeneous reaction in a catalytic layer attached to the duct wall may lead to concentration annulment along most of the surface of a monolith channel or microreactor. Fast reactions are natural candidates for microprocessing due to the fast heat removal and short residence time characteristics of these devices. Therefore, many processes involving microreactors and catalytic monoliths occur under external mass transfer control.[7] Recently, a criterion for attaining this regime was presented.[8] Alternatively, in the limit of a very slow reaction or when a biochemical reaction kinetics can be reasonably approximated by a zeroth-order reaction, Neumann's boundary condition is appropriate to describe the region where wall concentration exhaustion does not occur. Besides boundary conditions, the heat transfer problem shares similarity with the mass transfer one, i.e. the same equation describes concentration or temperature profiles made dimensionless according to

$$c = \frac{\hat{c}}{\hat{c}_{\text{in}}} \text{ or } T = \frac{\hat{T} - \hat{T}_{\text{wall}}}{\hat{T}_{\text{in}} - \hat{T}_{\text{wall}}} \tag{1}$$

The main quantity of interest is the mixing-cup concentration/temperature (velocity profile-averaged value over the

Correspondence concerning this article should be addressed to A. E. Rodrigues at arodrig@fe.up.pt.

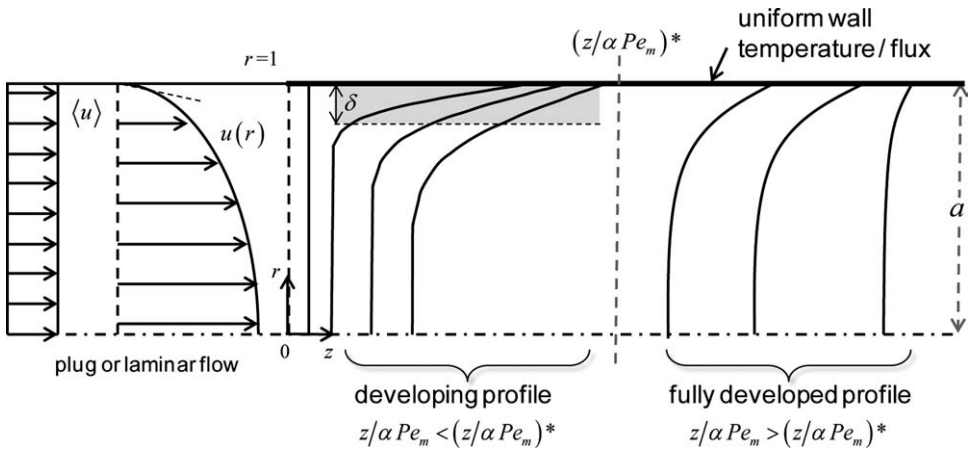

Figure 1. Schematic representation of the channel and of the concentration profile, according to a two-compartment model.

transverse length scale), since it describes the performance of the system (conversion) and can easily be measured experimentally (at least at the exit of the channel). From Graetz's series solution, the mixing-cup concentration profile is[3]

$$\langle T \rangle(z) \text{ or } \langle c \rangle(z) = \sum_{n=1}^{\infty} w_n \exp\left(\frac{-\lambda_n^2 z}{\alpha Pe_{m,\max}}\right) \tag{2}$$

where the coefficients w_n include integration constants and eigenfunction derivatives at the wall (related with Shah and London's G_n by $w_n = 2\sigma G_n/\lambda_n^2$), and λ_n are the eigenvalues associated to the eigenfunctions superposed in an infinite series (see Appendix). For Neumann and Dirichlet wall conditions, these quantities depend only on the channel geometry and on the (flat or parabolic) flow profile. Alternatively, one-dimensional models may be used, with heat or mass transfer coefficients calculated according to correlations for the Nusselt and Sherwood numbers of the form

$$Sh(z) = (S+1)\frac{k_m(z)a}{D} = \frac{-(S+1)\partial c/\partial r|_{\text{wall}}}{\langle c \rangle(z) - c_{\text{wall}}} = \frac{-(S+1)\sum_{n=1}^{\infty} A_n \varphi_n'(1)\gamma_n(z)}{\sum_{n=1}^{\infty} w_n \gamma_n(z) - \sum_{n=1}^{\infty} A_n \varphi_n(1)\gamma_n(z)}, \tag{3}$$

where $\gamma_n(z) = \exp\left(\frac{-\lambda_n^2 z}{\alpha Pe_{m,\max}}\right)$ is the part of the solution showing the dependence on the axial coordinate. From Eqs. 2 and 3, it is possible to see that an inconvenience occurs as $z/\alpha Pe_m \to 0$ in this slowly convergent series. In fact, the number of terms needed to obtain an accurate solution increase sharply as the inlet of the channel is approached or as convection becomes more dominant. In this case, the profile can be obtained by Lévêque's solution,[3,6,9,10] a simplified treatment concerned with the thin boundary layer that develops near the wall in the thermal entry region. In practical terms, the analysis of the problem in the whole range of Graetz number (αPe_m / z) has been fragmented into two main regions: an entrance length (where Lévêque's solution is valid) and a fully developed section (where only one term from the series in Eq. 2 is enough). Lévêque's regime and its transition to full development may be significant when millisecond contact time reactors are used, as it is often the case. Rosa et al.[11] reviewed the importance of several scaling effects in single-phase heat transfer in microchannels. They noted that several prior reviews have reported large discrepancies between experimental, rigorous numerical and analytical results. Then, several effects (arising from working at the microscale) that might be at the origin of such deviations were explored. Concerning inlet effects (development of the temperature profile), the following observations were made: (a) the thermal entry length solution must always be considered to describe heat transfer; (b) these effects can be especially important in microchannel sinks due to their compactness; (c) examination of the range of the Graetz parameter in several experimental works led to the conclusion that most of the times the profile cannot be considered fully developed. In the case of electrochemical microfluidic reactors, Yoon et al.[12] proposed an improved design based on the analysis of the boundary layer in the Graetz problem. They mention that many microreactors operate in the entrance length regime. Therefore, a non-negligible channel length may be required for the profile to be considered fully developed. A correct description of such cases has relied on the use of compartment models,[13,14] where once a critical value of $(\alpha Pe_m/z)^*$ is identified, Lévêque's solution is used if $\alpha Pe_m/z > (\alpha Pe_m/z)^*$, while the fully developed solution is adequate for $\alpha Pe_m/z < (\alpha Pe_m/z)^*$ (Figure 1). This represents a change from high to low conversion asymptotes as the Graetz parameter increases. It also represents the onset of diffusive effects at the global (maximum) transverse scale of the channel, as for $z/\alpha Pe_m < (z/\alpha Pe_m)^*$ these are confined in a boundary layer. When the profile is fully developed, transverse concentration gradients are important over the whole radius of the duct. In this case, a uniform value for Sherwood number is obtained.

A uniformly valid description of this fundamental problem has been pursued in several ways,[3] of which the most widely used are:

(a) Numerical calculation of w_n and λ_n ($n > 1$) to include more terms in Eq. 2: Brown[15] reports the first eleven terms in the solution for the Dirichlet problem in laminar flow. Other authors have tabulated eigenvalues and constants for several geometries (see Lopes et al.[16] and references therein).

(b) Calculation of w_n and λ_n using of asymptotic relationships for large n: Sellars et al.[17] use the WKB method to approximate eigenfunctions, eigenvalues and integration constants in Graetz's series solution. Newman[18] extended these

approximations, which were used by Shah and London[3] to estimate λ_n and G_n for $21 < n < 121$ for a circular channel.

(c) Matching of developed and developing profile limits by empirical correlations: This approach has been successfully applied to the prediction of *Sh* number as a function of the Graetz parameter. For example, Lopes et al.[8] provide expressions in the Dirichlet and Neumann limits.

(d) Extension of Lévêque's solution with higher order perturbation corrections: This has given origin to what is called Lévêque's series,[3] which is a perturbation series on powers of the concentration boundary layer thickness, δ

$$\langle c\rangle(z) = 1 - \sum_{n=0}^{\infty} \langle c\rangle_n \delta^n \tag{4}$$

where $\langle c\rangle_n(z) = -\frac{(S+1)}{\alpha\, Pe_m} \int_0^z \frac{d\, c_n}{d\, r}\big|_{\text{wall}}\, d\, z$ and $n \geq 1$. A reasonable number of terms in series (4) has been given by Newman[19,20] and Worsoe-Schmidt,[21] as reported in Shah and London[3] for both Dirichlet and Neumann boundary conditions. Note that from the convection-transverse diffusion dominant balance in the boundary layer, $\delta \sim [(S+3)\,\alpha\, Pe_m]^{-q}$, where: $q = 1/2$ for plug flow, $q = 1/3$ for laminar flow, $S = 0$ in a planar duct and $S = 1$ in a circular channel.

The following disadvantages or limitations of the previous approaches can be enumerated:

- It has been shown[22] that the evaluation of Graetz series terms with minimum associated error may have to include the use of strategies (a), (b), and (d) simultaneously, depending on the value of n and $z/\alpha\, Pe_m$, for the simpler case of uniform wall concentration (or temperature).
- A significant numerical effort may be associated with (a), since a large number of terms may be required. For example when $z/\alpha\, Pe_m > 10^{-4}$, Shah and London[3] used 120 terms in Eq. 2. Moreover, this gives origin to expressions far too complex with no insight on the contribution from the developing profile.
- An accurate approximation from Eq. 4 in the intermediate region demands a large number of terms in this series. For $z/\alpha\, Pe_m < 10^{-4}$, Shah and London[3] use 7 terms. The higher order terms are meant to account for the effects of channel curvature and velocity profile nonlinearity. Each coefficient is determined by solving a perturbation problem with subdominant terms that depend on solutions calculated previously. In addition, the approximation generally breaks down in the transition region.
- The formulation of empirical correlations may involve the introduction of fitting parameters to improve the approximation.[8]

In this work, we present an approximate solution for conversion ("Instantaneous concentration annulment at the wall" section) and for the Sherwood number ("Uniform wall mass/heat flux" section) which identifies both fully developed and developing profile contributions, requiring minimum numerical evaluation. This result accelerates the convergence rate of Graetz series producing only two or three terms. It is also free from the limitations of perturbation solutions (which require smallness of a parameter in the governing equations) as a result of the mathematical technique employed, which to our knowledge hasn't been applied to problems of this type so far. Moreover, criteria for the dominance of each contribution and transition between regimes will be provided ("Transition criteria between regimes" section). This is fundamental for the appropriate choice of correlations in the modeling and interpretation of experimental data. Our procedure consists in asymptotically evaluating the summations in Eqs. 2 and 3, rewritten as

$$Sh(z) \text{ or } \langle c\rangle(z) \sim \lim_{N\to\infty} \sum_{n=0}^{N} f(n) \tag{5}$$

for large N and for each of the geometries and flow profiles studied. This implies that each term in those summations will have to be written explicitly as a function of n. Even though this is only known exactly for the case of plug-flow between parallel plates, accurate solutions can be obtained with some additional assumptions.

Instantaneous Concentration Annulment at the Wall (or Uniform Wall Temperature)

In the case where transverse transport controls, estimates for the eigenvalues and weights in Eq. 2 can be analytically calculated in an approximate manner (the subscript ∞ denotes Dirichlet conditions). This is the case where the first weight $w_{1,\infty}$ deviates most from unity ($w_{1,\infty} \leq w_1 \leq 1$), and where subsequent coefficients decay more slowly (since $\sum w_n = 1$).

Asymptotic dependence of eigenvalues and coefficients

The values for the first eigenvalue can be obtained numerically and are widely tabulated[3,15,23]

$$\lambda_{1,\infty}^2 = \begin{cases} \pi^2/4 & \text{(parallel plates)} \\ 5.784 \sim 9\pi^2/16 & \text{(circular channel)} \end{cases} \text{ for plug flow,} \tag{6a}$$

$$\lambda_{1,\infty}^2 = \begin{cases} 2.828 & \text{(parallel plates)} \\ 7.313 & \text{(circular channel)} \end{cases} \text{ for laminar flow,} \tag{6b}$$

For laminar flows, the asymptotic predictions from Sellars et al.[17] for large eigenvalues (yielding $\lambda_{1,\infty} = 5/3$ and $\lambda_{1,\infty} = 8/3$, respectively) have less than 1% and 3% relative error in comparison with Eq. 6b.

The coefficients in Eq. 2 are given by

$$w_{n,\infty} = \frac{2(S+1)}{\lambda_{n,\infty}^2} \qquad \text{(plug flow)} \tag{7}$$

Note that $S = 0$ for parallel plates and $S = 1$ for a circular channel. When the flow profile is fully developed

$$w_{n,\infty} = 4\frac{3^{11/6}}{\sqrt{\pi}\Gamma(1/6)}\lambda_{n,\infty}^{-7/3} = 3.0384\lambda_{n,\infty}^{-7/3} \quad \text{(parallel plates)} \tag{8a}$$

$$w_{n,\infty} = 32\frac{3^{5/6}}{\sqrt{\pi}\Gamma(1/6)}\lambda_{n,\infty}^{-7/3} = 8.1023\lambda_{n,\infty}^{-7/3} \quad \text{(circular channel)} \tag{8b}$$

for $n = 1,2\ldots$. The above results were obtained from WKB theory for large eigenvalues,[17] nevertheless in the Dirichlet limit they are acceptable even for $n = 1$.[16] Numerical values for $w_{1,\infty}$ are also widely tabulated (Lopes et al.[16] and references therein).

Writing the terms in Eqs. 2 or 3 as $f(n)$ in Eq. 5 requires some assumptions concerning the spacing between λ_n and λ_{n+1} and the dependence of weights on eigenvalues. The key

assumption of our analysis is that the spacing between consecutive eigenvalues can be considered independent of n, i.e.

$$\lambda_{n,\infty} = \lambda_{1,\infty} + (n-1)\Delta\lambda \quad (n = 1, 2\ldots) \tag{9}$$

where for large eigenvalues, the uniform spacing is

$$\Delta\lambda = \begin{cases} \pi & \text{(plug-flow)} \\ 4 & \text{(laminar flow)} \end{cases} \tag{10}$$

When the flow profile is flat, this is exact for parallel plates, but only approximate for a circular channel, since the spacing between eigenvalues is $\Delta\lambda_{n,\infty} \sim \pi - 1/(8\pi n^2) + O(n^{-3})$ (i.e. becomes closer to π as $n \to \infty$) from the asymptotic expansion of Bessel functions.[24] For laminar flows, WKB theory for large eigenvalues predicts a value of $\Delta\lambda$ which is independent of the channel geometry (the curvature effects in the region next to the catalytic wall are $O(\lambda_n^{-2/3})$). Equations 7–10 allow us to express the coefficients in the mixing-cup concentration as

$$w_{n,\infty} = w_{1,\infty}\left(1 + \frac{\pi(n-1)}{\lambda_{1,\infty}}\right)^{-2} (n = 1, 2\ldots) \text{ (plug-flow)} \tag{11a}$$

$$w_{n,\infty} = w_{1,\infty}\left(1 + \frac{4(n-1)}{\lambda_{1,\infty}}\right)^{-7/3} (n = 1, 2\ldots) \text{ (laminar flow)} \tag{11b}$$

Coefficients and eigenvalues are now a function of n, requiring only the (exact or approximate) knowledge of $\lambda_{1,\infty}$ and $w_{1,\infty}$. Even though these simplifications hold more accurately as $n \to \infty$, we will consider them accurate enough as the basis to build our approximation.

Structure of the mixing-cup concentration/temperature profile

According to the previous section, the terms in the summation in Eq. 5 are now in appropriate form so that the asymptotic behavior of the sum as $N \to \infty$ can be determined using the Euler-Maclaurin sum formula.[25] Retaining the relevant terms, the simplified result for conversion of reactant X_R is obtained

$$X_R = 1 - \langle c \rangle \sim X_{GRAETZ} + X^*_{LEVEQUE} - HOT \tag{12}$$

The following contributions to the conversion profile along the channel can be identified:

- the first term of Graetz's solution is exactly of the same form as that in Eq. 2

$$X_{GRAETZ}(z) = 1 - w_{1,\infty}\exp\left(\frac{-\lambda_{1,\infty}^2\, z}{\alpha\, Pe_{m,\max}}\right) \tag{13}$$

with $\lambda_{1,\infty}^2$ and $w_{1,\infty}$ exactly known from Eqs. 6 or estimated by asymptotic methods;

- the modified Lévêque's solution, $X^*_{LEVEQUE}$ consists of Lévêque's solution multiplied by a corrective gamma function

$$X^*_{LEVEQUE} = \frac{1}{\Gamma(q)}\,\Gamma\left(q, \frac{\lambda_{2,\infty}^2\, z}{\alpha\, Pe_{m,\max}}\right) X_{LEVEQUE} \tag{14}$$

Note that $q = 1/2$ for plug flow, $q = 1/3$ for laminar flow and that the original Lévêque solution is given by[3,9,23]

$$X_{LEVEQUE}(z) = \frac{2(S+1)}{\sqrt{\pi}}\sqrt{\frac{z}{\alpha\, Pe_m}} \quad \text{(plug flow)} \tag{15a}$$

$$X_{LEVEQUE} = \frac{3^{4/3}\,(S+1)\,(S+3)}{2^{5/3}\,\Gamma(1/3)}\left(\frac{z}{\alpha\, Pe_{m,\max}}\right)^{2/3} \quad \text{(laminar flow)} \tag{15b}$$

with $S = 0$ for plates and $S = 1$ for circular channel;

- the second term of Graetz's solution multiplied by a compensation function Δ, which together with Eq. 14 accounts for the higher order terms (HOT) of Eq. 2 ignored in Eq. 13

$$HOT = w_{2,\infty}\,\Delta\,\exp\left(\frac{-\lambda_{2,\infty}^2\, z}{\alpha\, Pe_{m,\max}}\right) \tag{16}$$

In Eq. 16, the second eigenvalue is simply $\lambda_{2,\infty} = \lambda_{1,\infty} + \Delta\lambda$, and is associated with the weight $w_{2,\infty} (= w_{1,\infty}\,\lambda_{1,\infty}^2/\lambda_{2,\infty}^2$ e.g. for plug-flow). The function Δ appearing in Eq. 16 depends linearly on the reciprocal of the Graetz number ($z/\alpha Pe_m \sim Gz^{-1}$) and is defined as

$$\Delta = \Delta_1 + \Delta_2\frac{z}{\alpha\, Pe_{m,\max}} \tag{17}$$

By forcing the inlet boundary condition to be fulfilled, the coefficients in Eq. 17 can be calculated using only the first eigenvalue and previous relationships to yield

$$\Delta_1 = \frac{1 - w_{1,\infty}}{w_{2,\infty}} \tag{18a}$$

$$\Delta_2 = \frac{\Delta\lambda}{6}\,\lambda_{2,\infty} \tag{18b}$$

These results replace the earlier prediction in Eq. 19. Rigorously, the result obtained for Δ_1 can be shown to be associated with the corrective effect accounting for all weights ignored if series Eq. 2 is truncated after the second term, i.e. by application of the Euler-Maclaurin sum formula to

$\Delta_1 = \sum_{n=2}^{\infty} w_{n,\infty}/w_{2,\infty}$:

$$\Delta_1 = \frac{1}{2} + \frac{\pi}{6\,\lambda_2} + \frac{\lambda_2}{\pi} \quad \text{(plug flow)} \tag{19a}$$

$$\Delta_1 = \frac{1}{2} + \frac{7}{9\,\lambda_2} + \frac{3\,\lambda_2}{16} \quad \text{(laminar flow)} \tag{19b}$$

Equations 19 are the approximate statement that all coefficients add to 1, and therefore Δ_1 can be alternatively calculated from $\sum_{n=1}^{\infty} w_{n,\infty} = w_{1,\infty} + w_{2,\infty}\,\Delta_1 = 1$. Each term in Eq. 12 is plotted as a function of $z/\alpha Pe_m$ in Figure 2 for a

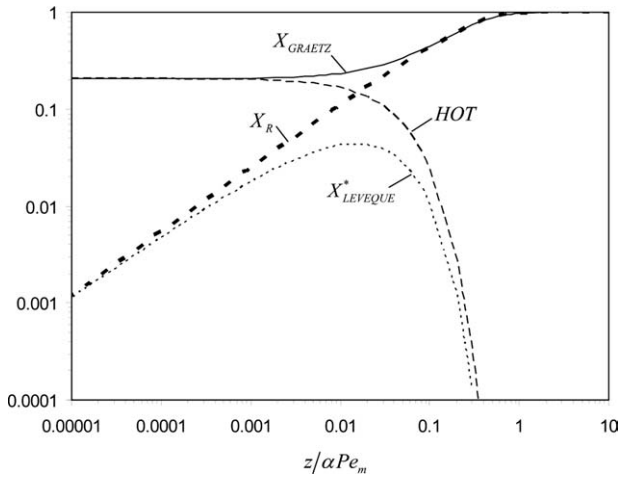

Figure 2. Conversion X_R as a function of the reciprocal of Graetz number ($z/\alpha Pe_m$) in an infinitely long circular channel with Dirichlet wall boundary condition, according to Eq. 12.

The contributions of the one-term Graetz solution X_{GRAETZ}, the higher order terms HOT and the corrected Lévêque solution ($X^*_{LEVEQUE}$) are also plotted as given by Eqs. 13–16.

catalytic tubular reactor with parabolic velocity profile. The behavior of the different contributions in Eq. 12 is qualitatively the same for both geometries and flow profiles.

For laminar flows, Shah and London[3] calculated the mixing-cup temperature profile under these conditions with the 120-term Graetz series (with both numerically and asymptotically determined eigenvalues and coefficients) for $z/\alpha Pe_m > 10^{-4}$ and with the 7-term Lévêque series from Worsoe-Schmidt[21] for $z/\alpha Pe_m < 10^{-4}$. In a circular channel, the maximum error of Eq. 12 compared to Graetz series is 0.09% at $z/\alpha Pe_m = 0.1$ (in the intermediate regime between the developing and fully developed limits), as shown in Figure 3. For higher $z/\alpha Pe_m$, the relative error decays sharply, as the concentration tends to zero. If $z/\alpha Pe_m < 6 \times 10^{-5}$, in the range where Lévêque's extended solution is more appropriate, the relative error is below 3×10^{-4} %, while the deviation from Graetz series solution increases due to the unsuitability of that solution in the entry region. Increasing the number of terms in the series, increases the range where Graetz solution is still a correct estimate, but it is a slowly convergent series: agreement with 5 digits between Eq. 2 with 10 and 120 terms only occurs for $z/\alpha Pe_m > 0.02$. For lower $z/\alpha Pe_m$, the error in using Graetz series increases significantly, and so does the error compared to solution Eq. 12. Equation 12 has also several advantages over existing solutions from 1D models with coefficients fitted from comparison with particular numerical results. Since the latter are not based on a uniform solution, but only on the asymptotes, they usually result in a compartmented solution with several ranges of Graetz parameter and significant higher error at the endpoints of each interval.

Qualitatively, the behavior of the error between approximation Eq. 12 and Graetz and Lévêque's series is identical in a planar duct or when the velocity profile is flat. The maximum deviations from Graetz series are: 0.1% at $z/\alpha Pe_m = 0.10$ for plug-flows and 2.6% for laminar flow between parallel plates at $z/\alpha Pe_m = 0.01$. The relative error with Graetz's series (for higher values of $z/\alpha Pe_m$) and with Lévêque's series (for lower values of $z/\alpha Pe_m$) decreases sharply. Nevertheless, the intermediate region is also well described by Eq. 12, with low errors from numerical calculations or from Lévêque's extended solution.

Concerning the degree of development of the profile, we observe that the weighing function $\Gamma(q,\lambda^2_{2,\infty}\, z/\alpha Pe_{m,\max})/\Gamma(q)$ in Eq. 14 is related to the fraction of the profile described by the inlet asymptote. If the value of this function is set to 1%, then $z/\alpha Pe_m = 0.12$ (laminar flow in a circular channel). If 10%, $z/\alpha Pe_m = 0.04$. Then, depending on the level of influence from inlet effects that we are willing to tolerate, the value of the Graetz parameter can be calculated accordingly.

Uniform wall mass/heat flux

When the mass or heat flux at the wall can be considered uniform, the boundary condition at the wall becomes

$$\left.\frac{\partial c}{\partial r}\right|_{r=1} = f \tag{20}$$

where in the mass transfer problem, $f = 0$ for a channel with inert wall (in the limit of a very slow heterogeneous reaction) or $f = -Da$ if a zeroth-order reaction occurs (without wall concentration annulment). The mixing-cup concentration (or temperature) is given by[3,26,27]

$$\langle c \rangle = 1 + f\,\frac{\sigma\, z}{\alpha\, Pe_{m,\max}} \qquad \text{(plug and laminar flow)} \tag{21}$$

Contrary to the previous case with Dirichlet boundary condition, $\langle c \rangle$ in Eq. 21 does not include contribution from the entry length profile. However, while in the uniform wall concentration situation little insight is obtained by looking at the Sherwood number, here it is useful to analyse this quantity in more detail. We define Sh_H (or Nu_H, for simplicity both noted as Sh) as

$$Sh = \frac{-(S+1)\,f}{\langle c \rangle(z) - c(r=1,z)} \tag{22}$$

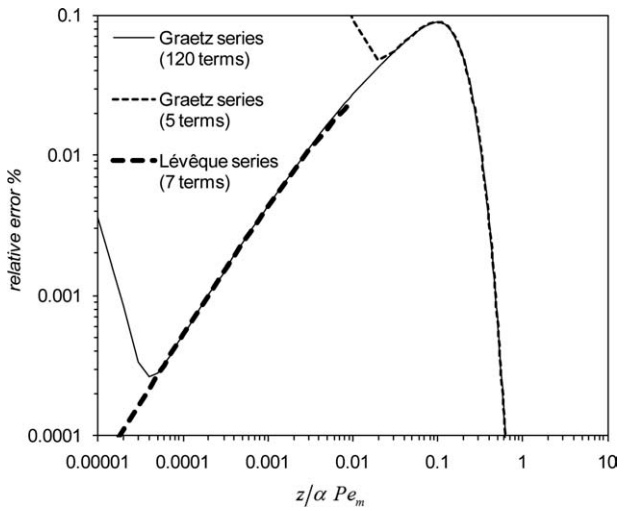

Figure 3. Relative error of the improved solution (12) with Graetz series (2) (with 5 and 120 terms) and with Lévêque's series (4) with 7 terms as described in Shah and London.[3]

This refers to laminar flow inside a circular channel.

Considering the full solution for the wall concentration $c(r = 1, z)$[26,27]

$$\frac{1}{Sh} = \frac{1}{Sh_{\text{fd}}} + \sum_{n=1}^{\infty} \frac{A_{n,0}\ \varphi_n(1)}{(S+1)}\ \exp\left(\frac{-\lambda_{n,0}^2\ z}{\alpha Pe_{m,\max}}\right) \tag{23}$$

where: Sh_{fd} is the fully developed value of Sherwood number given by Eqs. 24 below, $A_{n,0}\ \varphi_n\ (1)$ is the product of the eigenfunction evaluated at the wall and the integration constant for the homogeneous eigenvalue problem in Neumann conditions and $\lambda_{n,0}$ is the associated eigenvalue, evaluated as described in the next section. For both planar ($S = 0$) and circular channels ($S = 1$)

$$Sh_{\text{fd}} = (S+3)(S+1) \qquad \text{(plug-flow)} \tag{24a}$$

$$Sh_{\text{fd}} = \frac{(S+1)(S+5)(S+7)}{5\ S+17} \qquad \text{(laminar flow)} \tag{24b}$$

Asymptotic dependence of eigenvalues and coefficients

We will assume again that eigenvalues are equally spaced according to Eq. 9. From the same asymptotic behavior (large eigenvalues), $\Delta\lambda$ takes the same values for flat ($\Delta\lambda = \pi$) and parabolic ($\Delta\lambda = 4$) profiles, for both geometries. The first eigenvalue is given by[3,17]

$$\lambda_{1,0}^2 = \begin{cases} \pi^2 & \text{(parallel plates)} \\ 14.6819 & \text{(circularchannel)} \end{cases} \qquad \text{(plug flow)} \tag{25a}$$

$$\lambda_{1,0}^2 = \begin{cases} 18.3801 & \text{(parallel plates)} \\ 25.6796 & \text{(circular channel)} \end{cases} \qquad \text{(laminar flow)} \tag{25b}$$

Concerning the dependence of $A_{n,0}\ \varphi_n\ (1)$ on $\lambda_{n,0}$, it can be shown that $-A_{n,0}\ \varphi_n\ (1) = 2\ \lambda_{n,0}^{-2}$ for plug-flows and $-A_{n,0}\ \varphi_n\ (1) \sim 2.401006045\ \lambda_{n,0}^{-5/3}$ for laminar flows (approximately for high eigenvalues). The numerically calculated values for $n = 1$ are[3]

$$-A_{1,0}\ \varphi_1(1) = \begin{cases} 0.20264 & \text{(parallel plates)} \\ 0.136222 & \text{(circular channel)} \end{cases} \qquad \text{(plug flow)} \tag{26a}$$

$$-A_{1,0}\ \varphi_1(1) = \begin{cases} 0.2222280 & \text{(parallelplates)} \\ 0.19872216 & \text{(circularchannel)} \end{cases} \qquad \text{(laminarflow)} \tag{26b}$$

Uniformly valid approximation to Sherwood/Nusselt number

Obtaining an uniform solution in this case involves the asymptotic evaluation of the summation in Eq. 23, which can be written as $\sum_{n=0}^{N} f(n)$ as $N \to \infty$. We apply the Euler-Maclaurin sum formula[25] to obtain

$$\sum_{n=1}^{\infty} \frac{A_{n,0}\ \varphi_n(1)}{(S+1)}\ \exp\left(\frac{-\lambda_{n,0}^2\ z}{\alpha Pe_{m,\max}}\right) = \frac{\Theta_{\text{LEV}}}{Sh_{\text{LEV}}} + \text{HOT} \tag{27}$$

Concerning Eq. 27, the following remarks should be made:

- Lévêque's leading-order solution for Sherwood's number, Sh_{LEV}, is given by

$$Sh_{\text{LEV}} = \frac{\sqrt{\pi}}{2}\ (S+1)\sqrt{\frac{\alpha Pe_m}{z}} \qquad \text{(plug flow)} \tag{28a}$$

$$Sh_{\text{LEV}} = 0.820199\ (S+1)\left(\frac{\alpha Pe_{m,\max}}{z}\right)^{1/3} \text{(laminarflow)} \tag{28b}$$

- As before, Lévêque's term appears multiplied by a corrective gamma function

$$\Theta_{\text{LEV}} = \frac{1}{\Gamma(1-q)}\ \Gamma\left(1-q, \frac{\lambda_{2,0}^2\ z}{\alpha Pe_{m,\max}}\right) \tag{29}$$

- the higher-order terms HOT that result from the asymptotic summation are written as

$$\text{HOT}(S+1) = A_{1,0}\ \varphi_1(1)\ \exp\left(\frac{-\lambda_{1,0}^2\ z}{\alpha Pe_{m,\max}}\right) + A_{2,0}\ \varphi_2(1)\ \left(\Delta_1 + \Delta_2\ \frac{z}{\alpha Pe_{m,\max}}\right)\ \exp\left(\frac{-\lambda_{2,0}^2\ z}{\alpha Pe_{m,\max}}\right) \tag{30}$$

where HOT < 0 and

$$\Delta_1 = -\frac{A_1\ \varphi_1(1)}{A_2\ \varphi_2(1)} - \frac{S+1}{A_2\ \varphi_2(1)\ Sh_{\text{fd}}} \tag{31a}$$

$$\Delta_2 = \frac{\Delta\lambda\ \lambda_{2,0}}{6} \tag{31b}$$

The values for Δ_1 were calculated so that the inlet boundary conditions are fulfilled (this substitution is consistent as shown previously).

$A_{2,0}\ \varphi_2\ (1)$ and $\lambda_{2,0}$ are calculated from $A_{1,0}\ \varphi_1\ (1)$, $\lambda_{1,0}$ and the assumption of equally spaced eigenvalues. Moreover, $q = 1/2$ for plug flow, $q = 1/3$ for laminar flow, $S = 0$ for a planar duct and $S = 1$ for a circular channel, as before.

Substituting Eq. 27 in 23, yields

$$\frac{1}{Sh} = \frac{\Theta_{\text{fd}}}{Sh_{\text{fd}}} + \frac{\Theta_{\text{LEV}}}{Sh_{\text{LEV}}} \tag{32}$$

where $\Theta_{\text{fd}} = 1 + \text{HOT}\ Sh_{\text{fd}}$, since the existence of higher-order terms is a measure of the importance of the fully developed contribution. For laminar flow inside a circular channel, the dependence of Θ_{fd} and Θ_{LEV} on $z/\alpha Pe_m$ is shown in Figure 4. Correlations based on the addition of both developing and fully developed limits are frequently used (e.g., in Lopes et al.[8]). Equation 32 provides a justification for the form of such approximations, with additional functions that weigh the importance of each contribution.

The Sherwood number can be calculated as described in Shah and London,[3] using both Graetz (with numerical and asymptotic data) and Lévêque's series. For a circular channel with parabolic velocity profile, Figure 5 compares these results with Eq. 32. In this case, the modulus of the relative error compared with Eq. 32 has a maximum of 4% at $z/\alpha Pe_m = 0.04$ (corresponding to $\sim$0.236 in absolute error), as shown in Figure 6. The error is reduced if a planar

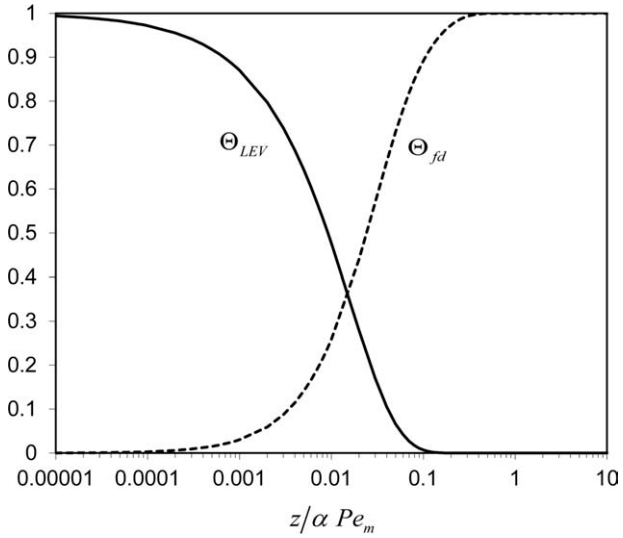

Figure 4. Θ_{fd} and Θ_{LEV} as functions of $z/\alpha Pe_m$ for laminar flow inside a circular channel.

channel is considered (maximum of 1.2% at $z/\alpha Pe_m = 0.03$) or if the velocity profile is flat (e.g., maximum of 0.114% for $z/\alpha Pe_m = 0.03$ in a circular channel).

Transition criteria between regimes and ranges of validity

In the previous sections, we identified the contributions from the entry length and fully developed solutions as a result of the asymptotic technique employed. We now use these results to derive criteria for delimiting regimes.

Dirichlet boundary condition

As we have shown previously, the fully developed contribution (X_{GRAETZ}) can be isolated from the other terms in the uniformly valid approximation Eq. 12. Therefore, a suitable criterion for evaluating the degree of convective dominance is given by

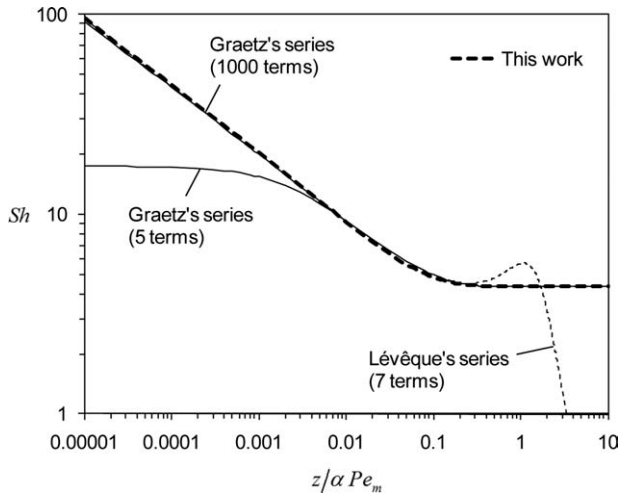

Figure 5. Sherwood number (*Sh*) as a function of $z/\alpha Pe_m$ for laminar flow inside a circular channel with uniform wall flux.

The result from this work, Eq. 32, is compared with the solution from Graetz's series (with 5 and 1000 terms) and with the 7-term Lévêque's series from Shah and London.[3]

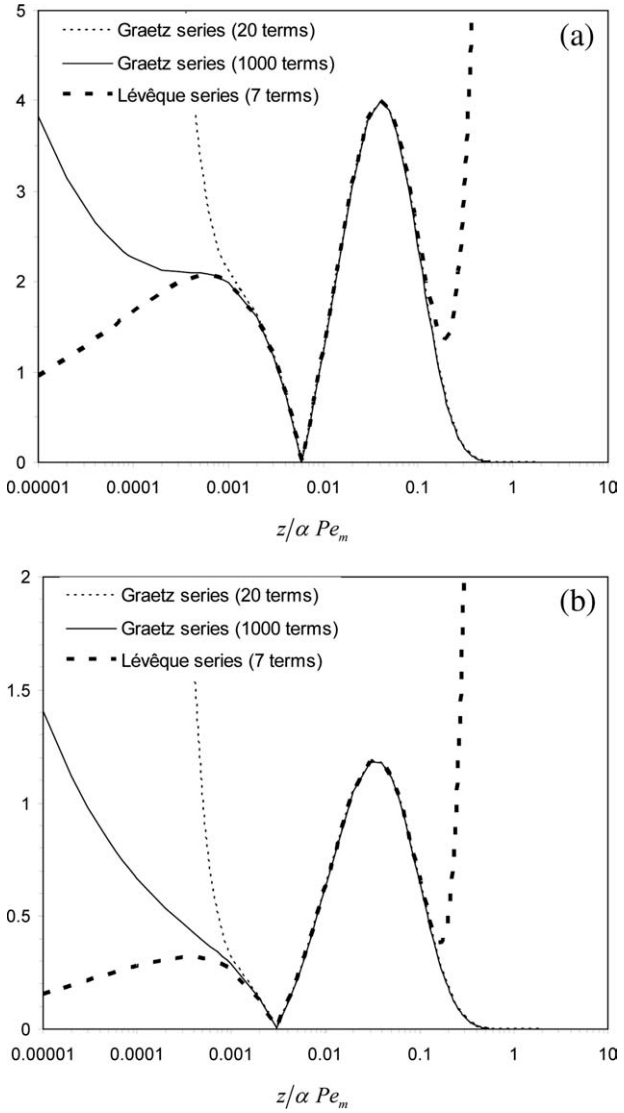

Figure 6. Relative error involved in estimating the Sherwood/Nusselt number with Eq. 32, in a circular (a) or planar (b) channel with Neumann wall boundary condition and laminar flow.

Comparison of Graetz series (with either 20 or 1000 terms) and with Lévêque's series (7 terms) as given by Shah and London[3] is shown.

$$\varphi = \frac{X_{\mathrm{GRAETZ}} - X_R}{X_{\mathrm{GRAETZ}}} \tag{33}$$

Equivalently, Eq. 33 expresses the degree of transverse transport control and it is written as the sum of all higher order terms, normalized by the 1-term solution for conversion of reactant. According to the form of our approximate solution for X_{R}, Eq. 12

$$\varphi \sim \frac{\mathrm{HOT} - X^*_{\mathrm{LEVEQUE}}}{X_{\mathrm{GRAETZ}}} \tag{34}$$

Taking into account the dependence of each term in Eq. 34 on the Graetz number (Figure 2), we note that: when $X_{\mathrm{R}} \rightarrow X_{\mathrm{GRAETZ}}$, $\varphi \rightarrow 0$ (since HOT $\sim X^*_{\mathrm{LEVEQUE}} \rightarrow 0$ and $X_{\mathrm{GRAETZ}} \sim O(1)$) and when $X_{\mathrm{R}} \rightarrow X_{\mathrm{LEVEQUE}}$, $\varphi \rightarrow 1$ (since

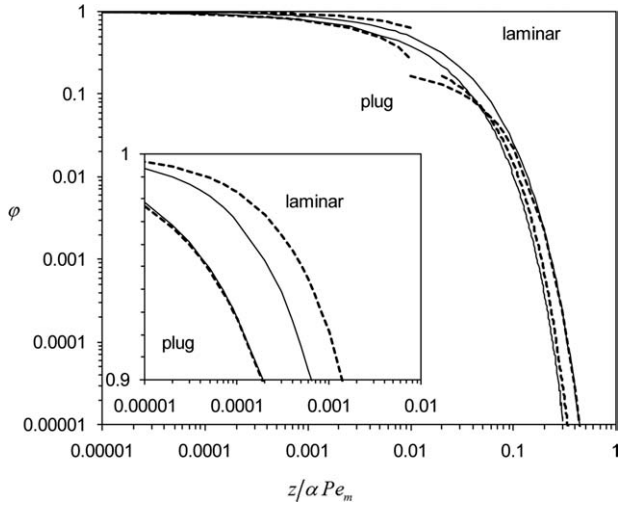

Figure 7. Degree of transverse transport control in a circular channel with Dirichlet wall boundary condition.

The full lines were calculated according to the uniformly valid approximation Eq. 12. The limiting forms of the criterion (Eqs. 36 and 37 given by dashed lines) agree reasonably for $\varphi \to 1$ and $\varphi \to 0$. Both plug and laminar flows are considered.

$X_{\mathrm{GRAETZ}} \sim$ HOT, while $X^{*}_{\mathrm{LEVEQUE}} \sim X \to 0$). Therefore, φ is bounded and changes from 0 to 1 as $\alpha Pe_m/z$ increases from 0 to ∞. Equation 34 may be accurately evaluated with the results presented earlier (plotted in Figure 7 for flow in a circular channel). For a given value of φ, the resulting (nonlinear) expression must be solved for $z/\alpha Pe_m$. Since our purpose is to derive the boundaries that delimit the regions where conversion can be confidently estimated by either X_{GRAETZ} or X_{LEVEQUE}, we are interested in the two asymptotes of Eq. 34: $\varphi \to 1$ and $\varphi \to 0$.

For plug-flow, expanding Eq. 34 around $z/\alpha Pe_m = 0$ or simply taking $X_{\mathrm{R}} \to X_{\mathrm{LEVEQUE}}$ in Eq. 33 and expanding around the same point yields

$$\frac{z}{\alpha Pe_m} \le \frac{\pi}{4}\left(\frac{1-w_{1,\infty}}{S+1}\right)^2 (1-\varphi)^2 \qquad \text{(entrance length as } \varphi \to 1\text{)} \quad (35)$$

Similarly for laminar flow, the critical value of the reciprocal of the Graetz parameter below which Lévêque's approximation can be used is

$$\frac{z}{\alpha Pe_{m,\max}} \le \frac{1.3778}{(S+3)^{1/2}}\left(\frac{1-w_{1,\infty}}{S+1}\right)^{3/2}(1-\varphi)^{3/2} \qquad \text{(entrance length as } \varphi \to 1\text{)} \quad (36)$$

For the derivation of a criterion for the applicability of the one-term Graetz regime, we consider: $w_{1,\infty}\exp(-\lambda^2_{1,\infty} z/\alpha Pe_{m,\max}) < 1$, $X^{*}_{\mathrm{LEVEQUE}} \to 0$ but $\Delta_1 \gg \Delta_2\, z/\alpha\, Pe_{m,\max}$. This set of assumptions leads to

$$\frac{z}{\alpha\, Pe_{m,\max}} \ge \frac{1}{\lambda^2_{2,\infty}} \ln\left(\frac{1-w_{1,\infty}}{\varphi}\right) \qquad \text{(fully developed regime as } \varphi \to 0\text{)} \quad (37)$$

valid for plug and laminar flows. Figure 7 shows the φ curve vs. the reciprocal of Graetz number for a circular channel. Equations 36 and 37 are able to predict the result from Eq. 34 with the uniform approximation outlined in the "Structure of the mixing-cup concentration profile" section. For parallel plates, the agreement for $\varphi \to 1$ improves because there is no need to account for channel curvature. Plug-flow cases are also better described since no linearization of the velocity profile near the wall is introduced.

Concerning the above criteria, we can make the following remarks:

(a) The variation in the value of $z/\alpha Pe_m$ in Figure 7 is more abrupt in the range where the Graetz solution is adequate. This results in a bigger insensitivity to the criteria in this regime, whereas in the definition of the applicability of Lévêque's solution, the arbitrarily fixed value of φ may induce large changes in the entrance length.

(b) The influence of the flow profile in the fully developed boundary is irrelevant. There are numerical difficulties associated with the limit of $\varphi \to 0$ (near zero concentrations), therefore Eq. 37 is particularly useful.

(c) The value of φ can be directly related with the relative error that occurs when estimating conversion from the one-term Graetz solution

$$\varepsilon_{\mathrm{GRAETZ}} = (X_{\mathrm{GRAETZ}} - X_{\mathrm{R}})/X_{\mathrm{R}} = \varphi/(1-\varphi) \sim \varphi \quad (38)$$

(d) The error that results from using Lévêque's approximation Eq. 15 is given by $\varepsilon_{\mathrm{LEV}} = |X_{\mathrm{LEV}} - X_{\mathrm{R}}|/X_{\mathrm{R}}$, which in the limit of $z/\alpha Pe_m \to 0$ relates with φ according to

$$\varepsilon_{\mathrm{LEV}} = \frac{\pi}{4}\, w_{1,\infty}\, \lambda^2_{1,\infty}\, \frac{1-w_{1,\infty}}{(S+1)^2}\, (1-\varphi)^2 \sim (1-\varphi)^2 \text{ (plug flow)} \quad (39a)$$

$$\varepsilon_{\mathrm{LEV}} = 1.3778\, \frac{w_{1,\infty}\, \lambda^2_{1,\infty}\, \sqrt{1-w_{1,\infty}}}{(S+3)^{1/2}\,(S+1)^{3/2}}\, (1-\varphi)^{3/2} \sim (1-\varphi)^{3/2} \text{ (laminar flow)} \quad (39b)$$

From Eq. 39, we can see that the error related with Lévêque's solution is more sensitive to the choice of φ, compared with Eq. 38. Also, the selection of the same value of φ for plug and laminar flows results in a more conservative criterion for the former.

(e) Depending on the agreement required mainly with Lévêque's original solution, the transition region may extend by several orders of magnitude of $z/\alpha Pe_m$.

These results define the length of the intermediate region between developing and fully developed profile regimes. Operation and design in this range are of practical interest and haven't been sufficiently characterized. We have described analytically the transition from the low conversion (small temperature change, $\varphi \to 1$) asymptote to the high conversion one ($\varphi \to 0$). The same region marks the transition from low to high pressure drop regimes

$$\Delta P \Big/ \rho\langle u\rangle^2 \sim (\alpha\, Pe_m)^{-1} \sim \begin{cases} (1-\varphi)^{3/2}, & \varphi \to 1 \\ -\ln\,\varphi\ , & \varphi \to 0 \end{cases}$$

It is likely that an appropriate trade-off between achieving the required conversion/temperature difference at the minimum pressure drop yields an optimum point in the gap

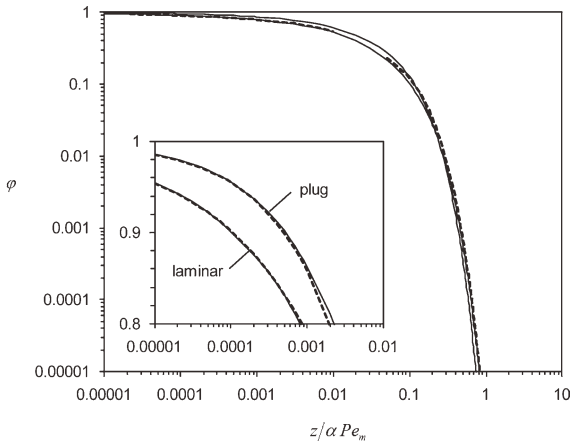

Figure 8. Degree of transverse transport control in a circular channel with Neumann wall boundary condition.

The full lines were calculated using Eq. 32. The dashed lines are given by the limiting forms for $\varphi \to 1$ and $\varphi \to 0$ in Eqs. 42 and 43. Both plug and laminar flows are considered.

between the two well-described limits. The penalty in conversion so that pressure drop decreases by a certain amount is related to the value of φ, as this measures the degree of agreement with the high conversion (fully developed) asymptote. The simple and accurate results provided can be used in optimization procedures, where many evaluations would be required. This may be particularly useful on the simulation of multi-channel systems, at the integrated reactor level.

Another well-known trade-off occurs between conversion and mass transfer. The effect of an entrance region is to increase the mass/heat transfer rate, compared to the fully developed region, even though this is detrimental to the overall conversion. This increment can be quantified in several ways (e.g. the incremental heat transfer number $N(z)$ given in Shah and London[3]). Therefore, $\boldsymbol{\varphi}$ also represents the increment in the transfer rate due to the influence of the inlet and the effect being privileged (high mass transfer rates $\boldsymbol{\varphi} \to 1$, or high conversions $\boldsymbol{\varphi} \to 0$). Setting $\boldsymbol{\varphi} = 0.01$ corresponds to allowing the transfer rate at a given position to be influenced by the inlet by 1%.

Neumann boundary condition

When the flux is uniform throughout the channel, we have separated developing and fully developed contributions in the correlation for Sherwood (or Nusselt) number, Eq. 32. In this case, a measure for profile development can be written as

$$\varphi = \frac{Sh - Sh_{\text{fd}}}{Sh} = \frac{1/Sh_{\text{fd}} - 1/Sh}{1/Sh_{\text{fd}}} \tag{40}$$

If $Sh > Sh_{\text{fd}}$ (as it happens in the entrance length), then $\varphi \to 1$. The fully developed region is characterized by low values of φ (since $\varphi \to 0$ as $Sh \to Sh_{\text{fd}}$). According to Eq. 32

$$\frac{\varphi}{Sh_{\text{fd}}} = -\text{HOT} - \frac{\Theta_{\text{LEV}}}{Sh_{\text{LEV}}} \tag{41}$$

which can be completely determined with the information in the "Uniformly valid approximation to Sherwood number" section. This is plotted as a function of $z/\alpha Pe_m$ for a circular channel in Figure 8. As previously, the limiting forms of Eq. 41 are

$$\frac{z}{\alpha Pe_m} \le \frac{\pi(S+1)^2}{4}\frac{(1-\varphi)^2}{Sh_{\text{fd}}^2}$$

(entrance length as $\varphi \to 1$ for plug flow) (42a)

$$\frac{z}{\alpha Pe_{m,\max}} \le 0.55177(S+1)^3\frac{(1-\varphi)^3}{Sh_{\text{fd}}^3}$$

(entrance length as $\varphi \to 1$ for laminar flow) (42b)

$$\frac{z}{\alpha Pe_{m,\max}} \ge \frac{1}{\lambda_{1,0}^2}\ln\left(\frac{-A_{1,0}\,\varphi_1(1)}{S+1}\frac{Sh_{\text{fd}}}{\varphi}\right)$$

(fully developed regime as $\varphi \to 0$) (43)

valid for plug and laminar flows. The calculation of Eq. 41 from the uniformly valid solution and the limiting forms Eqs. 42 and 43 are shown in Figure 8 for a circular channel. In the fully developed limit, the curves for plug and laminar flow overlap. The form of the curve in Figure 8 is similar to the one in Dirichlet case (previous section) and therefore the same comments are appropriate. Equation 40 directly measures the deviation of the actual Sherwood number from its fully developed value. On the other hand, the relative error associated with Eqs. 28 is given by

$$\varepsilon_{\text{LEV}} = \frac{Sh - Sh_{\text{LEV}}}{Sh} = \frac{1/Sh_{\text{LEV}} - 1/Sh}{1/Sh_{\text{LEV}}} \sim 1 - \Theta_{\text{LEV}} \tag{44}$$

Expanding Eq. 44 for $z/\alpha Pe_m \to 0$,

$$\varepsilon_{\text{LEV}} \sim \frac{1}{\Gamma(1-q)\,(1-q)}\left(\frac{\lambda_{2,0}^2\, z}{\alpha Pe_m}\right)^{1-q}$$

Substituting Eq. 42, ε_{LEV} can be related with φ:

$$\varepsilon_{\text{LEV}} \sim (S+1)\frac{\lambda_{2,0}}{Sh_{\text{fd}}}(1-\varphi) \sim (1-\varphi) \text{ (plug flow)} \tag{45a}$$

$$\varepsilon_{\text{LEV}} \sim 0.745201(S+1)^2\frac{\lambda_{2,0}^{4/3}}{Sh_{\text{fd}}^2}\,(1-\varphi)^2 \sim (1-\varphi)^2 \text{ (laminar flow)} \tag{45b}$$

For the same value of φ, the criterion is more conservative for laminar flows.

Another interpretation of these results can be given in terms of the mass/thermal boundary layer developing near the interface. The thickness of this region δ is related to the Graetz parameter and it has been shown that it should be included e.g. in the criteria for delimitation of mass transfer – reaction regimes in a microreactor.[8,28] As in the case of the thermal/mass entrance length, there is a lot of disparity in the definitions and values reported concerning δ.

In the case of uniform wall flux, we have obtained an explicit approximation for the Sherwood/Nusselt number. From the theory of interphase transfer coefficients, we define the thickness of the boundary layer ($a\ \delta$) so that the mass/heat transfer coefficient is given by $k_m \sim D/(a\ \delta)$. Thus, the Sherwood/Nusselt number can be written as $Sh(z)$

$= (S + 1)/\ \delta(z)$. The maximum boundary layer thickness is $\delta_\infty = (S + 1)/Sh_{\mathrm{fd}}$. The normalized thickness so that $\delta^* = 1$ (boundary layer thickness equals the radius of the channel) for fully developed profile is

$$\delta^* = \frac{Sh_{\mathrm{fd}}}{Sh}$$

Introducing Eq. 32 or 40

$$\delta^* = \Theta_{\mathrm{fd}} + \frac{Sh_{\mathrm{fd}}}{Sh_{\mathrm{LEV}}}\ \Theta_{\mathrm{LEV}} = 1 - \varphi$$

In the case of a Dirichlet wall boundary condition, our criterion φ was formulated in terms of conversion values, which makes the relationship with Sherwood number more complex. For simplicity, and since we are looking for an estimate, the following expression is proposed

$$\delta^* \sim (1 - \varphi)^{q/(1-q)}$$

where $q = 1/2$ for plug and $q = 1/3$ for laminar flow. This allows both fully developed and developing dependences of δ^* on the Graetz parameter to be respected. The exact numerical coefficients may differ a little from this estimate, but the correct order of magnitude is kept. We note that according to Equations 39 at the inlet: $\delta^* \sim \sqrt{\varepsilon_{\mathrm{LEV}}}$ for plug flow and $\delta^* \sim \varepsilon_{\mathrm{LEV}}^{1/3}$ for laminar flow. On the other hand, according to Eq. 38 when the profile is near full development: $\delta^* \sim 1\text{-}\varepsilon_{\mathrm{GRAETZ}}$ for plug flow and $\delta^* \sim \sqrt{1 - \varepsilon_{\mathrm{GRAETZ}}}$ for laminar flow. The correct estimation of this thickness is fundamental for the design of optimized microchannel systems, where the complete or a fraction of the boundary layer is removed or disrupted by the periodic placing of outlets or inlets.[12]

Expressing the dependence of Nusselt or Sherwood number on the Graetz parameter is often not achieved by a single expression. Almost all correlations for Sherwood/Nusselt number are given in branches with compartmented ranges of validity (usually, one for fully developed conditions and other(s) for developing profile), and one can find many examples of this in Shah and London's book.[3] Since each expression is constructed from asymptotic limits, it is recognized that at the intersection of both asymptotes or in the limits of each interval, the error in predicting Sherwood number is maximum. A curious consequence from Eq. 32 is an estimate for the maximum error associated with this approach. At the intersection: $Sh_{\mathrm{fd}} = Sh_{\mathrm{LEV}} = Sh_{\mathrm{est}}$ (estimated Sherwood number). Then, the relative error from this approach is given by

$$\mathrm{error} = 1 - \frac{Sh_{\mathrm{est}}}{Sh} = 1 - (\Theta_{\mathrm{fd}} + \Theta_{\mathrm{LEV}})$$

This should be evaluated at the intersection point, which are given in Table 1 (criterion type B). For laminar flow in a circular channel: error ~9%. In this case, the existence of an uniformly valid solution to the interphase coefficient can reduce the error significantly.

From Figure 4, we can observe that Θ_{fd} and Θ_{LEV} intersect at $z/\alpha Pe_m \sim 0.01$ at a value of ~0.4. At this point, $\varphi \sim 0.5$ which corresponds to the intermediate level of profile development. This validates the roles of Θ_{fd}, Θ_{LEV} and φ as being indicative of the degree of profile development.

Comparison with previous criteria

In most of the chemical engineering literature, the ranges of validity of the entrance and fully developed models have been obtained in a number of ways that we briefly detail below. Table 1 situates previous regime boundaries within our criterion by calculating the respective value of φ. Data from the following five "calculation methods" are presented:

A. *Analogy with the Momentum Boundary Layer Development Length.* For example, Kockmann[14] scale the entrance length for the concentration profile from the hydrodynamic length yielding in our variables

$$\frac{z}{\alpha\, Pe_m} \leq 0.05\ \frac{d_h^2}{a^2}$$

In Table 1, we compare this with other criteria for laminar flow in a channel with Dirichlet wall boundary condition.

B. *Intersection of Fully Developed and Lévêque Asymptotes in a $Sh - \alpha\, Pe_m/z$ Plot.* Lopes et al.[8] calculated the value of the Graetz parameter where Lévêque's correlation attained the fully developed value. This is a usual procedure, which however ignores the intermediate region. In this case, transition occurs around $\varphi \sim 0.10$.

C. *Error Comparison with Numerical Solution.* Gervais and Jensen[13] determined the intersection of absolute error curves from 1D models with developing and fully developed correlations for *Sh*. Their result for laminar flow between parallel plates with symmetric boundary conditions is in Table 1.

D. *Agreement with Sh_{fd} by an Arbitrarily Defined Margin of Error.* The reference book from Shah and London[3] presents the distance required to achieve a local Nusselt number equal to 1.05 of the fully developed temperature profile value. Polyanin et al.[29] also calculate the length of the thermal initial region so that $Nu = 1.01\ Nu_{\mathrm{fd}}$. Table 1 contains these results for laminar flow. It can be seen directly in the case of Neumann boundary condition, that our criteria confirms these results.

E. *Agreement Between Analytical Solutions.* Shah and London[3] give the range of $z/\alpha Pe_m$, where the Nusselt number calculated from the 120-term Graetz series equals the one from the 7-term Lévêque series up to 5 or more digits. In addition, Alonso et al.[30] identified the transition region in laminar flow inside a circular channel with wall concentration annulment ($0.05 \leq z/\alpha\, Pe_m \leq 0.2$). This is also included in Table 1 for comparison.

From these few examples in the literature, we can make the following comments:

(a) As expected, most available information refers to the value of the Graetz parameter below which the fully developed profile is adequate. Much less information concerning the validity of Lévêque's solution is provided. The finite transition region between both regimes is also frequently ignored.

(b) There is a large variation in the boundaries that are provided, sometimes by one-order of magnitude. This is reflected in terms of φ values, and consequently on the relative error incurred by the use of approximations (see e.g. Eqs. 38 and 39).

(c) When provided, the boundary for the developing profile given by Lévêque's solution is usually overestimated (values of φ not high enough).

Despite this and the fact that the concept of thermal/mass profile development length is well established, it is a common practice to propose criteria for the negligibility of

Table 1. Comparison of the Ranges of Validity Given in the Literature with Our Criteria

Shape	Flow Profile	Boundary Condition	Criterion Type	$\frac{z}{\alpha\, Pe_m}$	φ	Refs.
Circular	Laminar	Dirichlet	A	0.2	0.002	14
						30
			B	0.1021	0.03	8
			D	0.22	0.001	29
				0.1339	0.01	3
			E	$>8 \times 10^{-5}$	0.974	
				<0.02	0.315	
				>0.05	0.108	30
		Neumann	B	0.1063	0.09	8
			D	0.28	0.01	29
				0.722	0.04	3
			E	$>8 \times 10^{-4}$	0.80	
				<0.02	0.40	
	Plug	Dirichlet	B	0.0381	0.10	8
		Neumann	B	0.0491	0.27	
Plates	Laminar	Dirichlet	A	0.8	$\sim 10^{-9}$	14
			B	0.07	0.07	8
			C	0.24	0.001	13
			D	0.01276	0.014	3
			E	>0.008	0.58	
				<0.016	0.43	
		Neumann	B	0.0948	0.14	8
			D	0.1847	0.045	3
			E	>0.008	0.57	
				<0.08	0.17	
	Plug	Dirichlet	B	0.0523	0.1	8
		Neumann	B	0.0873	0.26	

entrance effects with no relationship to the arbitrary basis on which they were formulated and without the information that the analytical solution provides. Instead, an order of magnitude for the Graetz parameter is often preferred. Recently, Morini[31] proposed that inlet effects on the average Nusselt number can be neglected if $Gz = \langle u \rangle d_h^2/(DL) < 10$. From Figure 7, we can see that this corresponds to $(\alpha\ Pe_m)^{-1} > 0.4$ and to a very conservative (low) value of φ. Order of magnitude results ignore the correct numerical coefficients, which distinguish different shapes and flow conditions.

We note that in principle the analysis can be extended to channels with different cross-sectional shapes. From WKB theory for large eigenvalues, curvature is negligible at the region near the interface, and therefore the dependence of eigenvalues and weights on n should be approximately the same. The correct values for λ_1 and w_1 can be calculated numerically or taken from the literature[3,4] for many geometries. Lévêque's solution can also be extended using a normalization based on the friction factor.[3] At the convective dominated regime, shape effects are negligible at the boundary layer and it is only required to include the correct linearization for the laminar velocity profile. The same applies to other Graetz problems that have appeared in the literature[32–36] and received the same analytical treatment, as long as an asymptotic description of coefficients is available.

Conclusions

We have derived an approximate analytical solution to Graetz's problem in terms of a combination of the fully developed and developing (Lévêque's) limits. Our solutions for the mixing-cup concentration/temperature profile or for Sherwood number, as a function of the axial distance, have the following features: (a) accurate results are obtained over the full range of the Graetz number ($\alpha\ Pe_m/z$); (b) relative error does not increase sharply in any specific range; (c) both limiting regimes are respected and the gap between them is well described; and (d) the form of the analytical solution is much simpler than any of the existing (involving a large number of terms with numerically determined coefficients) and minimum numerical evaluation is required. Mixing-cup concentrations are described with a maximum of 0.1% relative error (except for laminar flow between parallel plates, where the error is higher but still tolerable). When the wall boundary condition is of Neumann type, a solution for the Sherwood number based on adding the entrance length and fully developed terms is given. Each term has an associated weighting function, for which analytical expressions are provided.

Finally, we define criteria for transition between regimes which reflect the relative errors obtained by using the fully developed or Lévêque solutions. Explicit expressions for the length of the profile development zone are provided as a function of a desired degree of agreement with the fully developed solution, channel geometry, flow profile and boundary condition type. Previous disperse results in the literature are framed in a common analysis. Ranges of validity for the developing profile asymptote are given, as well as estimates for the length of the transition region. The approach presented can be extended to the analysis of Graetz or other chemical engineering problems.

Acknowledgments

J.P. Lopes gratefully acknowledges the financial support from Fundação para a Ciência e a Tecnologia (FCT), PhD fellowship SFRH/BD/36833/2007.

Notation

a = radius of the circular channel or half-spacing between parallel plates
A_n = nth integration constant

c = bulk fluid concentration of reactant species
$\langle c \rangle$ = reactant's mixing-cup concentration of the reactant species
c_{in} = inlet reactant concentration
D = bulk fluid diffusivity
d_h = hydraulic diameter
Da = Damköhler number for a zero-order reaction
G_n = coefficients used by Shah and London[3] in the mixing-cup temperature profile ($= -A_n/2d\varphi_n/dr|_{r=1}$)
HOT = higher order terms
k_m = interphase transfer constant
L = length of the channel
Pe_m = transverse Peclet number ($= a\langle u \rangle/D$ or $= a\langle u \rangle/\kappa$)
q = exponent in Lévêque's dependence on Graetz's parameter
r = dimensionless transverse coordinate ($= \hat{r}/a$)
S = shape parameter: =0 for parallel plates; = 1 for circular channel
Sh = Sherwood number
T = temperature of the fluid
$\langle T \rangle$ = mixing-cup temperature of the fluid
$u(r)$ = velocity profile inside the channel
$\langle u \rangle$ = average velocity inside the channel
$v(r)$ = dimensionless velocity profile, normalized by average velocity
X_R = conversion of reactant
w_n = n^{th} coefficient related with Shah and London's[3] notation by $= 2\sigma G_n/\lambda_n^2$
z = dimensionless axial coordinate
$z/\alpha\, Pem$ = reciprocal of Graetz's parameter

Greek letters

α = aspect ratio of the channel
Δ = compensation function
$\Delta\lambda$ = spacing between eigenvalues
ε = relative error
δ = thickness of the concentration/thermal boundary layer
$\Gamma(z)$ = Gamma function, $\int_0^\infty t^{z-1}\, e^{-t}\, dt$
$\Gamma(a, z)$ = incomplete Gamma function, $\int_z^\infty t^{a-1}\, e^{-t}\, dt$
γ = axial contribution to terms in Graetz's solution
κ = thermal diffusivity
φ = degree of transverse transport control
φ_n = n^{th} eigenfunction
λ_n = n^{th} eigenvalues
σ = shape/flow parameter, $(S + 1)u_{max}/\langle u \rangle$

Superscripts

$\hat{}$ = dimensional quantity
$'$ = derivative

Subscripts

fd = fully developed
In = inlet
GRAETZ = Graetz series (1 term)
LEV = Lévêque's solution
max = maximum (referred to maximum velocity)
surf = at the wall of the channel
wall = at the wall of the channel
0 = in the Neumann limit
∞ = in the Dirichlet limit

Literature Cited

1. Graetz L. Ueber die Wärmeleitungsfähigkeit von Flüssigkeiten. *Annal Phys Chem*. 1883;18:79–94.
2. Nusselt W. Die Abhängigkeit der Wärmeübergangszahl von der Rohrlänge. *Z Vereines deutscher Ingenieure*. 1910;54:1154–1158.
3. Shah RK, London AL. *Laminar flow forced convection in ducts*. In: Irvine TF Jr, Hartnett JP, editors. *Advances in Heat Transfer. Supplement 1*. New York: Academic Press, 1978.
4. Kays WM, Crawford ME. *Convective Heat and Mass Transfer*, 2nd ed. New York: McGraw-Hill, 1980.
5. Bejan A. *Convection Heat Transfer*. 1st ed. New York: Wiley, 1984.
6. Weigand B. *Analytical Methods for Heat Transfer and Fluid Flow Problems*. Berlin: Springer, 2004.
7. Kreutzer MT, Kapteijn F, Moulijn JA. Shouldn't catalysts shape up? Structured reactors in general and gas-liquid monolith reactors in particular. *Catal Today*. 2006;111:111–118.
8. Lopes JP, Cardoso SSS, Rodrigues AE. Multiscale analysis of a coated-wall microchannel reactor: Criteria for kinetic and mass transfer control with isothermal first-order reaction. In: XIX International Conference on Chemical Reactors—CHEMREACTOR-19. Boreskov Institute of Catalysis: Vienna, Austria, 2010.
9. Lévêque MA. Les lois de la transmission de chaleur par convection. *Ann Mines*. 1928;13:201–299.
10. Rice RG, Do DD. *Applied Mathematics and Modeling for Chemical Engineers*. New York: Wiley, 1995.
11. Rosa P, Karayiannis TG, Collins MW. Single-phase heat transfer in microchannels: the importance of scaling effects. *Appl Therm Eng*. 2009;29:3447–3468.
12. Yoon SK, Fichtl GW, Kenis PJA. Active control of the depletion boundary layers in microfluidic electrochemical reactors. *Lab Chip Mini Chem Biol*. 2006;6:1516–1524.
13. Gervais T, Jensen KF. Mass transport and surface reactions in microfluidic systems. *Chem Eng Sci*. 2006;61:1102–1121.
14. Kockmann N. *Transport phenomena in micro process engineering*. In: Mewes D, Mayinger F, editors. *Heat and Mass Transfer*, 1st ed. Berlin: Springer-Verlag, 2008.
15. Brown GM. Heat or mass transfer in a fluid in laminar flow in a circular or flat conduit. *AIChE J*. 1960;6:179–183.
16. Lopes JP, Cardoso SSS, Rodrigues AE. Approximate calculation of conversion with kinetic normalization for finite reaction rates in wall-coated microchannels. *AIChE J*. 2011; in press, DOI: 10.1002/aic.12483.
17. Sellars J, Tribus M, Klein J. Heat transfer to laminar flow in a round tube or flat conduit—the Graetz problem extended. *ASME Trans*. 1956;78:441–448.
18. Newman J. *The Graetz problem*. In: Bard AJ, editor. *The Fundamental Principles of Current Distribution and Mass Transport in Electrochemical Cells*. New York: Dekker, 1973:187–352.
19. Newman J. Extension of the Leveque solution. *J Heat Transf*. 1969;91:177–178.
20. Newman JS. *Electrochemical Systems*, 1st ed. Englewood Cliffs, NJ: Prentice-Hall, 1973.
21. Worsoe-Schmidt PM. Heat transfer in the thermal entrance region of circular tubes and annular passages with fully developed laminar flow. *Int J Heat Mass Transf*. 1967;10:541–551.
22. Housiadas C, Larrodé FE, Drossinos Y. Numerical evaluation of the Graetz series. *Int J Heat Mass Transf*. 1999;42:3013–3017.
23. Carslaw HS, Jaeger JC. *Conduction of Heat in Solids*, 2nd ed. New York: Oxford University Press, 1959.
24. Abramowitz M, Stegun IA. *Handbook of Mathematical Functions*, 10th ed. Washington, D.C.: National Bureau of Standards, 1972.
25. Bender CM, Orszag SA. *Advanced Mathematical Methods for Scientists and Engineers*. New York: McGraw-Hil, 1978.
26. Siegel R, Sparrow EM, Hallman TM. Steady laminar heat transfer in a circular tube with prescribed wall heat flux. *Appl Sci Res*. 1958;7:386–392.
27. Bauer HF. Diffusion, convection and chemical reaction in a channel. *Int J Heat Mass Transf*. 1976;19:479–486.
28. Lopes JP, Cardoso SSS, Rodrigues AE. Criteria for kinetic and mass transfer control with isothermal first-order reaction in a coated-wall microchannel reactor. *Chem Eng J*. 2011; DOI: 10.1016/j.cej.2011.05.088.
29. Polyanin AD, Kutepov AM, Vyazmin AV, Kazenin DA. *Hydrodynamics, mass and heat transfer in chemical engineering*. In: Hughes R, editor. *Topics in Chemical Engineering*. London: Taylor & Francis, 2002.
30. Alonso M, Alguacil FJ, Huang CH. Analytical approximation to the fully developed concentration profile of diffusive aerosol particles in laminar flow in a circular tube. *J Aerosol Sci*. 2010;41:413–417.
31. Morini GL. Scaling effects for liquid flows in microchannels. *Heat Transf Eng*. 2006;27:64–73.
32. Aydin O, Avci M. On the constant wall temperature boundary condition in internal convection heat transfer studies including viscous dissipation. *Int Commun Heat Mass Transf*. 2010;37:535–539.
33. Haji-Sheikh A, Beck JV, Amos DE. Axial heat conduction effects in the entrance region of circular ducts. *Heat Mass Transf*. 2009;45:331–341.
34. Ray S, Misra D. Laminar fully developed flow through square and equilateral triangular ducts with rounded corners subjected

to H1 and H2 boundary conditions. *Int J Therm Sci*. 2010; 49:1763–1775.
35. Vera M, Liñán A. Exact solution for the conjugate fluid-fluid problem in the thermal entrance region of laminar counterflow heat exchangers. *Int J Heat Mass Transf*. 2011;54:490–499.
36. Weigand B, Gassner G. The effect of wall conduction for the extended Graetz problem for laminar and turbulent channel flows. *Int J Heat Mass Transf*. 2007;50:1097–1105.
37. Damköhler G. Einfluss von diffusion, Strömung, und Wärmetransport auf die Ausbeute in Chemisch-Technischen Reaktionen. *Chem Eng Tech*. 1937;3:359–485.

Appendix: Graetz-Nusselt Problem

The governing equations that describe the classical Graetz problem include transport in a channel by convection in the axial direction and transverse diffusion. For a circular channel, the mass (or heat) balance writes as

$$\frac{1}{r}\frac{\partial}{\partial r}\left(r\frac{\partial c}{\partial r}\right) = \alpha Pe_m\, v(r)\,\frac{\partial c}{\partial z} \tag{A1}$$

where the dimensionless independent variables are the axial position scaled by the channel length ($z = \hat{z}/L$) and the transverse position within the open channel (normalized by channel radius ($r = \hat{r}/a$)). Concentration or temperature are normalized according to Eq. 1. The dimensionless uniform and parabolic velocity profiles are

$$v(r) = \frac{u(r)}{\langle u\rangle} = \begin{cases} \frac{S+3}{2}(1-r^2) & \text{laminar flow} \\ 1 & \text{plug-flow} \end{cases} \tag{A2}$$

where $S = 0$ for parallel plates and $S = 1$ for circular channel.

The two dimensionless parameters in Eq. A1 are: the transverse mass Péclet number ($Pe_m = \langle u\rangle a/D$) and the channel aspect ratio ($\alpha = a/L$). Axial diffusion is negligible up to $O(\alpha^2)$, i.e. for small aspect ratio channels. In this case ($\alpha \ll 1$), the inlet Danckwerts' boundary condition is simplified to uniform inlet concentration for $Pe_m \gg \alpha$

$$c(r,0) = 1 \tag{A3}$$

In the transverse direction, the symmetry boundary condition is appropriate at $r = 0$. Additionally, a condition at the wall is required. In the case of a microchannel reactor where a first-order reaction is occurring at the wall it writes as

$$\left.\frac{\partial c}{\partial r}\right|_{r=1} = -Da\; c(1,z) \tag{A4}$$

where the Damköhler number ($Da = ak_{\text{obs}}/D$) accounts for the reaction timescale. In this work, we are concerned with two particular limits of (A4): $Da \to 0$ and $Da \to \infty$, Neumann and Dirichlet boundary conditions respectively. For the heat transfer problem, Eq. A4 expresses finite wall thermal resistance[3] (R_{wall}), where the same limiting forms are found for $R_{\text{wall}} \to \infty$ and $R_{\text{wall}} \to 0$. The well-known solution[1,37] to this problem has the following separable form

$$c(r,z) = \sum_{n=1}^{\infty} A_n\; \varphi_n(r)\; \exp\left(\frac{-\lambda_n^2}{\alpha\, Pe_{m,\max}} z\right) \tag{A5}$$

where $\varphi_n(r)$ is an eigenfunction in the transverse coordinate, while the exponential term represents the axial dependence of the concentration profile (being $Pe_{m,\max}$ the transverse Péclet number evaluated at the maximum velocity in the channel). Averaging this equation over the channel's transverse length, with the velocity profile, yields Eq. 2.

Manuscript received Feb. 18, 2011, and revision received May 10, 2011.